

Available online at [www.sciencedirect.com](http://www.sciencedirect.com)**ScienceDirect**Journal homepage: [www.elsevier.com/locate/cortex](http://www.elsevier.com/locate/cortex)**Special issue: Research report****The architecture of mammalian cortical connectomes in light of the theory of the dual origin of the cerebral cortex**

Alexandros Goulas <sup>a,\*</sup>, Daniel S. Margulies <sup>b</sup>, Gleb Bezgin <sup>c</sup> and Claus C. Hilgetag <sup>a,d</sup>

<sup>a</sup> Institute of Computational Neuroscience, University Medical Center Hamburg-Eppendorf, Hamburg University, Hamburg, Germany

<sup>b</sup> Centre National de la Recherche Scientifique (CNRS) UMR 7225, Frontlab, Institut du Cerveau et de la Moelle épinière, Paris, France

<sup>c</sup> McConnell Brain Imaging Centre, Montreal Neurological Institute, McGill University, Montreal, QC, Canada

<sup>d</sup> Department of Health Sciences, Boston University, Boston, MA, USA

**ARTICLE INFO****Article history:**

Received 29 May 2018

Reviewed 30 July 2018

Revised 4 January 2019

Accepted 5 March 2019

Published online 13 March 2019

**Keywords:**

Wiring principles

Transcriptome

Comparative connectomics

Organizational axis

Unifying principles

**ABSTRACT**

Uncovering organizational principles of the cerebral cortex is essential for proper understanding of this prominent structure of the mammalian brain. The theory of the dual origin of the cerebral cortex offers such organizational principle. Here, we demonstrate that a duality pertains to the connectional architecture of the cerebral cortex of different mammals. This dual structure also constitutes a major axis of organization of the transcriptional architecture of the cortex and reflects the expression of different morphogens stemming from distinct patterning centers in the developing pallium. The duality of the cortex is also reflected in its spatial dimension, highlighting cortical areas as spatially ordered constellations that are centered around the paleocortex and archicortex, with the later primordial moieties reminiscent of antipodal points in the cortical sheet. The ontogeny of the uncovered dual connectional structure might be rooted in heterochronous neurodevelopmental gradients in the developing pallium, a suggestion corroborated by computational modeling. In all, the current results exemplify the duality of the cerebral cortex as an overarching organizational principle, reflected across the different levels of cortical architecture of different mammalian species, defining a natural axis of mammalian cortical organization.

© 2019 Elsevier Ltd. All rights reserved.

\* Corresponding author. Institute of Computational Neuroscience, University Medical Center Hamburg-Eppendorf, Hamburg University, Martinistra. 52, 20246, Hamburg, Germany.

E-mail address: [a.goulas@uke.de](mailto:a.goulas@uke.de) (A. Goulas).

<https://doi.org/10.1016/j.cortex.2019.03.002>

0010-9452/© 2019 Elsevier Ltd. All rights reserved.

## 1. Introduction

Understanding the organization of the cerebral cortex requires uncovering the fundamental principles pertaining to its architecture. Like the rings of a tree, the cerebral cortex consists of rings of progressive laminar differentiation emanating from two sources, that is, the piriform cortex (paleocortex) and the hippocampus (archicortex). These dual sources of differentiation of the cortex constitute the basic premise of the dual origin theory of the cerebral cortex (Fig. 1). The concept of the dual nature of the cerebral cortex can be traced back at least to the first decades of the last century and has been observed in reptiles, marsupials, monotremes, human and non-human primates (Shellshear, 1929; Dart, 1934; Abbie, 1940, 1942; Sanides, 1962, 1970) (Fig. 1). The dual origin of the cerebral cortex has been primarily inferred from cytoarchitectonic and myeloarchitectonic analysis. Cortical areas are parts of two gradients (or trends) of progressive laminar differentiation. Criteria for defining such gradients can include the progressive appearance and successive thickness and

neuronal density of layer IV and the overall more pronounced laminar differentiation, that is, distinguishability of cortical layers, as well as increased overall myelination. In sum, in the dual origin framework, cortical areas can be conceptualized as waves of laminar differentiation emanating from two origins, that is, the piriform cortex (paleocortex) and the hippocampus (archicortex) (Fig. 1).

The concept of the dual origin of the cerebral cortex was adopted and further expanded through a series of cytoarchitectonic and tract-tracing studies in the macaque monkey cortex by Pandya and co-workers (e.g., Pandya, Seltzer, & Barbas, 1988; Barbas & Pandya, 1989; Cipolloni & Pandya, 1999; Morecraft, Cipolloni, Stilwell-Morecraft, Gedney, & Pandya, 2004; for a review see Pandya & Yeterian, 1985; Pandya, Petrides, Seltzer, & Cipolloni, 2015). These foundational studies offer two fundamental insights concerning the macaque monkey cortex. First, the widely used dorsal/ventral dichotomy of sensory systems and lobes in the macaque monkey, e.g., in the visual (Ungerleider & Mishkin, 1982) and sensorimotor systems (Pandya et al., 1988) or the prefrontal cortex (Barbas & Pandya, 1989), is actually a snapshot of the

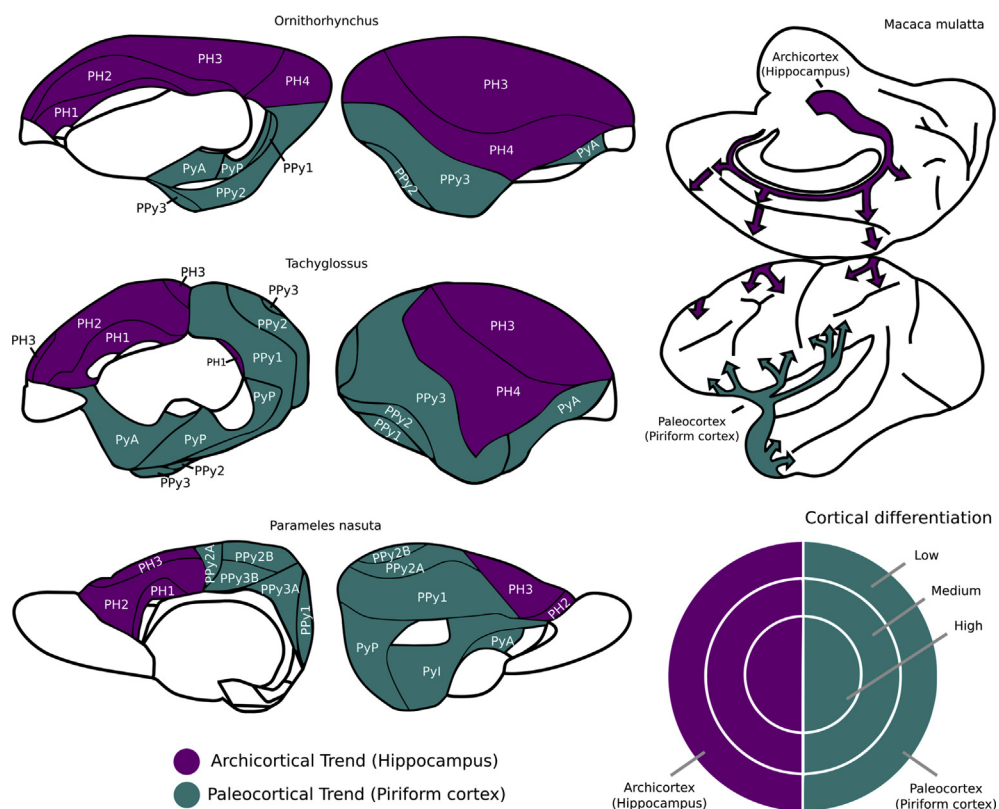


**Fig. 1 – Dual origin of the cerebral cortex of mammals based on cytoarchitectonic analysis.** Cortical maps depicting the duality of the cerebral cortex in various mammals. The duality of the cerebral cortex in these species is uncovered based on the step-wise cytoarchitectonic differentiation of the cerebral cortex. This step-wise laminar differentiation is depicted with arrows in the macaque monkey cortex (top right), with the direction of the arrows denoting less to more laminar differentiation. Based on the dual origin framework, each cortical area is situated in two gradations, or trends, the paleocortical or archicortical gradations. The less differentiated areas of the archicortical and paleocortical trend is the hippocampus and the piriform cortex, respectively, and constitute the two origins from which the cortical gradients emanate. Thus, each trend is a sequence of less to more differentiated areas, arranged in a spatially ordered manner that can be summarized as gradients forming co-centric rings in the cortex (bottom right). Cortical maps modified from (Abbie, 1940, 1942; Pandya & Yeterian, 1985).

global dual origin architecture of the macaque monkey cortex. Second, the duality of the cortex is also mirrored in the organization of cortico-cortical connections, that is, cortical areas that are affiliated with one of the two trends are primarily connected with cortical areas of the same trend (Pandya & Veterian, 1985; for a thorough review, see Pandya et al., 2015).

More recently, the dual connectional architecture of the cortex was conceptualized as a topologically symmetric constellation of areas (Bezgin et al., 2014). This definition allows the explicit, quantitative, connectivity-based analysis of cortical areas within the dual origin framework and results from such approach align very well with cytoarchitectonic analysis demonstrating the duality of the cortex (Bezgin et al., 2014) (Fig. 2A,B). Specifically, this computational connectivity-based approach has uncovered a dual connectional organization for the auditory/prefrontal and visual systems of the macaque monkey, that is, the dorsal and ventral streams of these systems, a division that aligns well with prior cytoarchitectonic, connectional and functional observations (Romanski et al., 1999; Ungerleider & Mishkin, 1982). Hence, the conceptualization and quantification of the dual architecture of the cortex as two topologically symmetric structures (or dual connectional trends) is offering a tool for examining the presence of such structure in other mammalian species.

The aforementioned studies revealed a duality of the cerebral cortex primarily on a cytoarchitectonic and connectional basis. Does the duality of the cerebral cortex constitute an organization axis of the transcriptional architecture of the cerebral cortex? Is this duality reflected in the physical layout of the cortical sheet? What are the plausible developmental mechanisms that result in such dual architecture? Such questions remain unanswered and are necessary to be addressed in order to understand the dual origin of the cerebral cortex at a more substantial level, elevate it to a key organizational principle of the mammalian cerebral cortex, and thus provide a framework that recapitulates the different levels of architecture of the mammalian cortex.

In the current study, we undertake this task. Specifically, we demonstrate, on a connectional basis and at a whole-cortex level, the existence of a dual architecture in the mouse, rat, cat, and macaque monkey cortex. We show that this dual architecture is reflected in the geometry of the cortical sheet, with the primordial areas of the dual trends reminiscent of antipodal points of the cortical sheet. We exploit recent detailed transcriptional data on the mouse cortex and show that the dual architecture is related to the transcriptional dimension of cortical organization. Lastly, we demonstrate, with the aid of computational modeling, that heterochronous development and connectivity formation in the cortex can give rise to the dual connectional architecture observed in the adult cerebral cortex.

We conclude that the duality of the adult cerebral cortex constitutes an organizational axis that epitomizes different levels of cortical organization. This duality is rooted in heterochronous neurodevelopmental events and encompasses multiple species across the mammalian spectrum, thus constituting a principle with a potentially universal scope.

## 2. Materials and methods

### 2.1. Macaque monkey

The macaque monkey connectome was based on Markov et al. (2014). As described in Markov et al. (2014), in total 29 cortical areas of the macaque monkey cortex were injected with retrograde tracers (diamidino yellow and fast blue). The M132 cortical atlas was used as a reference (Markov et al., 2014) for assembling the macaque monkey cortical connectome. The incoming connections from 91 areas covering the whole cortex were mapped. Specifically, projection neurons that have taken up the tracer were detected in each cortical area and the number of these neurons was tabulated. For each injection to a cortical area, the number of detected labeled neurons in each area was divided by the total number of neurons observed across the whole cortical sheet (excluding the injected area), thus giving rise to a normalized “strength” measure of connectivity, that is, the fraction of labeled neurons that are extrinsic to the injected area (FLNE). For the current study, we used the  $29 \times 29$  cortical connectome for which the status of every connection is known.

### 2.2. Mouse

The mouse connectome was based on Oh et al. (2014) and Zingg et al. (2014). These datasets offer information on the wiring of the whole extent of the mouse cerebral cortex. For the Oh et al. (2014) dataset, only intrahemispheric connections were considered, for consistency with the rest of the connectomes used in the current study. The dataset used for our main analysis is the Allen Mouse Connectivity Atlas (<http://connectivity.brain-map.org/>). The mouse wiring diagram was mapped by employing the recombinant adeno-associated virus expressing enhanced green fluorescent protein as an anterograde tracer. For constructing a large-scale connectivity map, the Allen Reference Atlas (<http://mouse.brain-map.org/static/atlas>) was used (Dong, 2008). In total 295 non-overlapping structures (cortical areas, subcortical nuclei etc.) were considered. Altogether 469 injected brains of C57BL/6J male mice were included in the construction of the large-scale connectivity matrix through constrained optimization. The constrained optimization sets about two thirds of all possible connections to zero (absent). The *p*-values were estimated for the remaining non-zero weights with linear regression (Oh et al., 2014). This procedure resulted in connectivity matrices involving 213 structures. Details on the informatics pipeline, quality controls and estimation of the inter-areal connectivity matrix are provided in Oh et al. (2014). The connectivity matrices from Oh et al. (2014) were obtained from the Open Connectome project (<http://www.openconnectomeproject.org/>). The .graphml file was converted to .gml with the online Open Connectome project conversion tools (<http://mrbrain.cs.jhu.edu/graph-services/convert/>). Lastly, the data from the .gml file were imported in Matlab and converted into a directed graph with the aid of Matlab scripts (<http://www.mathworks.de/matlabcentral/fileexchange/45741-read-gml>). We used 38 cortical areas for the mouse connectome. The

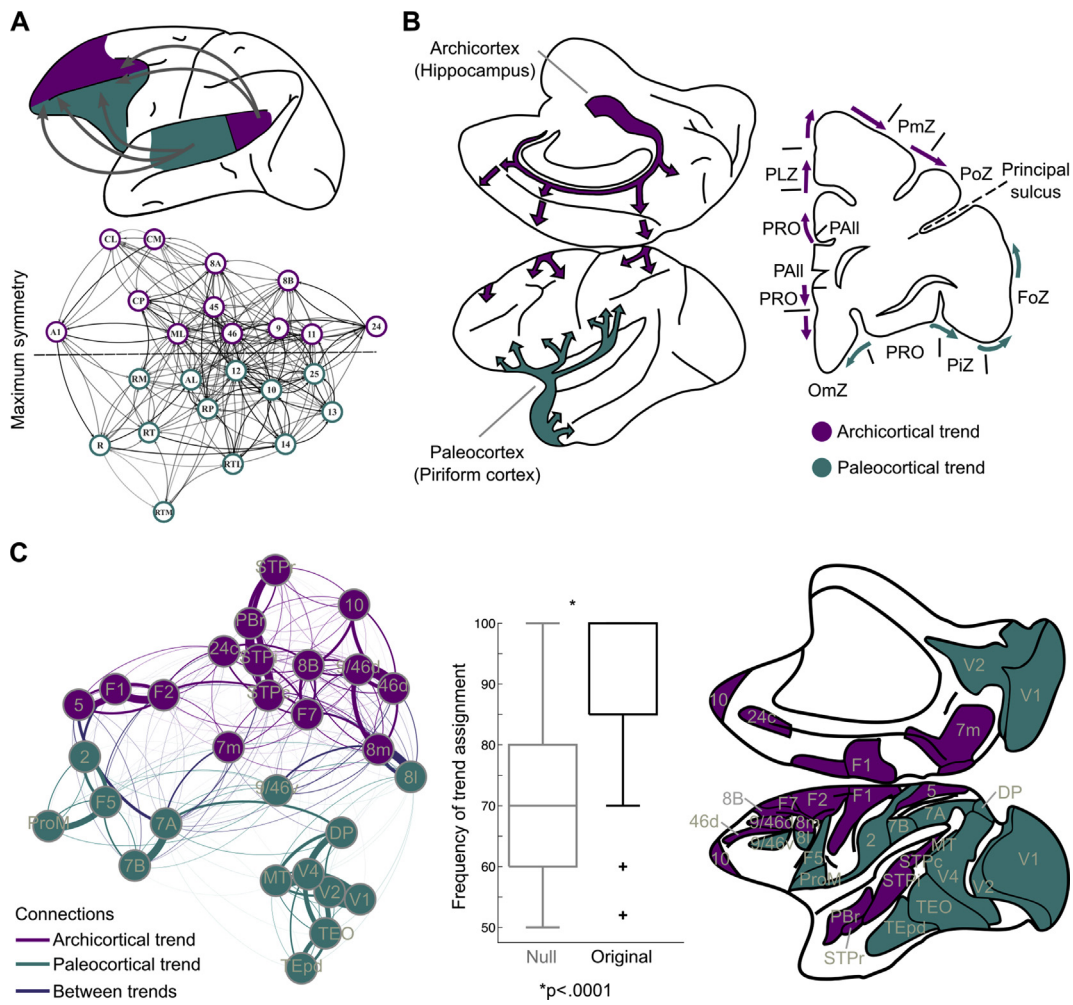


**Fig. 2 – Connectivity-based detection of the dual architecture in the macaque monkey.** A. Application of the dual connectional trends algorithm in the prefrontal-auditory connectional architecture (Bezgin et al., 2014). The algorithm splits the prefrontal and auditory areas in two topologically symmetric structures. This division corresponds to the division of these areas based on the dual origin framework (Pandya et al., 2015) (see also panel B). Hence, the conceptualization and quantification of the dual connectional trends of the cortex as two topologically symmetric structures is offering a tool for examining the presence of such structure at the whole-cortex level in other mammalian species. B. Schematic depiction of the dual architecture of the macaque monkey cerebral cortex based on its cytoarchitecture (Pandya et al., 2015; Sanides, 1970). Arrows depict the transition from less to more cytoarchitectonically differentiated parts of the cortex. Nomenclature depicted in the coronal section after Sanides (1970). PAII: Parietal cortex; PRO: Proisocortex; PLZ: Paralimbic zone; OmZ: Orbitomedial zone; PiZ: Parainsular zone; PmZ: Paramotor zone; PoZ: Paraopercular zone; FoZ: Frontopercular zone. Note the fusion of the two trends in the lateral surface, that is, at the principal sulcus and at the intraparietal sulcus. C. Results of the application of the dual connectional stream algorithm at a whole-cortex level. The derived dual connectional trends co-localize with the cytoarchitecture-based division proposed by the dual origin framework (Pandya et al., 2015) (Compare the connectivity-based division of areas with the division depicted in panel B). Note that the principal sulcus and the intraparietal sulcus are dividing the two trends in the lateral surface). 2D layout corresponds to a Kamada-Kawai force-directed drawing. The thickness of lines denotes the strength of connections, with thicker lines denoting stronger connections. From a statistical standpoint, the assignment of areas to the dual connectional trends is significantly more stable compared to a null model with preserved degree distribution and number of nodes and edges (statistical energy test). The distributions of the frequency of assignments for the null model corresponds to 100 null models. Nomenclature of cortical areas in panel C from (Markov et al., 2014). Cortical maps in panel B modified from (Pandya & Veterian, 1985; Sanides, 1970).

entorhinal cortex was excluded from the analysis, since not all of its sub-compartments were injected. Connections were considered present if they exhibited a  $p$ -value, obtained from the linear regression, below .05 and all remaining connections

were considered absent. The weight of the connections was not taken into account.

Importantly, the Oh et al. (2014) dataset contains large injections involving more than one cortical area and the

connectivity matrix relies on modeling assumptions that can lead to inaccurate estimation of cortico-cortical connections (Ypma & Bullmore, 2016). Therefore, we also used the Zingg et al. (2014) cortico-cortical connectivity dataset in order to assess the replication of the results in the mouse cortex. This dataset is derived from the combination of both anterograde (*phaseolus vulgaris* leucoagglutinin and dextran tetramethylrhodamine), as well as retrograde tracers (cholera toxin subunit b and Fluorogold). We used the logical AND between the connectivity matrices derived from anterograde and retrograde tracers, irrespective of connectivity strength. Therefore, a connection was considered present only if it was revealed as such by both anterograde and retrograde tracers. Thus, the Zingg et al. (2014) dataset constitutes a conservative estimation of cortico-cortical connections. Contrary to the Allen Mouse Connectivity Atlas, the Zingg et al. (2014) dataset was constructed from expert manual annotation, thus avoiding biases that can be introduced from modeling assumptions. An extra attractive feature of this dataset is that it also uses the Allen Reference Atlas as a reference atlas for assembling the mouse connectome. Small variations in the parcellation scheme used in the Oh et al. (2014) and Zingg et al. (2014) studies involve the subpartitioning of areas. For instance, Zingg et al. (2014) subpartition area SSs into a caudoventral and caudodorsal part. Such subpartitions were fused in one area, as well as their connections, in order to render the results from the two datasets comparable within the same parcellation scheme.

### 2.3. Rat

The rat cortico-cortical connectivity was estimated from the BAMS2 Workspace (Bota, Talpalaru, Hintiryan, Dong, & Swanson, 2014). We used the 2013 version of the rat connectome (R-BAMS-C 01 2013, January 2013). The database uses the Swanson (2004) nomenclature. This database is a collation of tract-tracing results from the literature, thus different types of tracers have been used. All connections that are deemed present in this database were taken into account irrespective of their strength.

### 2.4. Cat

The cat connectome was based on a meta-analysis of tract-tracing studies in the cat cortex (Scannell et al., 1995). This dataset is the only available whole-cortex cat connectome to date. Different nomenclatures were used for the different parts of the cortex, as well as different tract-tracers in each of the collated studies (Scannell et al., 1995).

### 2.5. Quantifying the dual connectional trends

We currently conceptualize the dual connectional architecture of the cerebral cortex as topologically symmetric structures (or trends) and quantify them accordingly. This conceptualization and subsequent quantification have led to divisions of the connectional architecture of the macaque monkey that correspond very well with known divisions, such as the dorsal and ventral connectivity streams of the visual and auditory-prefrontal systems (Bezgin et al., 2014). These

streams are snapshots of the global dual trends of the cerebral cortex (Pandya et al., 2015). Hence, in the present study, we use this conceptualization and quantification to uncover such duality in the connectional architecture of the macaque monkey at a global, whole-cortex level, as well as in other mammalian species. We should note that here the term “symmetry” denotes topological symmetry (see below) and not symmetry between the two hemispheres.

In order to detect the dual connectional trends of the cerebral cortex, the steps described in Bezgin et al. (2014) were followed. First, the nodes/areas of the connectome were projected to a 2D coordinate system. This was achieved with a force-directed algorithm (Fruchterman & Reingold, 1991). This algorithm uses attraction and repulsion forces with the former affecting only connected nodes/areas. After a random initialization of the node positions, the new position of each node is calculated based on the total repulsion and attraction with the rest of the nodes. This procedure, repeated multiple times (here set to 1000), results in a 2D arrangement of the nodes/areas so that connected areas tend to be spatially close. Second, the center of mass of the arrangement of areas in this 2D layout is calculated. A line passing through the center of mass splits the areas in two parts. The topological symmetry of the two parts is calculated as the average Mahalanobis distance of each node of one part with all the nodes of the other part. Third, the line passing through the center of mass of the 2D layout is rotated gradually, that is, 1° at each step. The process is repeated until a 180-degree rotation is completed. At each step, the symmetry of the two parts is calculated. The split with the minimum average Mahalanobis distance is selected. Due to the random initial positioning of the areas during the Fruchterman-Reingold algorithm, the whole procedure is repeated 100 times. The frequency of assignment of the areas to their respective connectional trends across the 100 applications of the algorithm results in a “consistency measure” of the split. We will refer to the two derived splits as dual connectional trends.

For the very dense macaque monkey connectome, accompanied by detailed quantitative information on the weight of the connections, a projection to the 2D space was performed with the Kamada-Kawai algorithm (Kamada & Kawai, 1989). The weights of the connections, that is the FLNe values (Markov et al., 2014), were transformed logarithmically and the negative values of this transformation were taken into account for computing the weighted paths between the nodes/areas. After the application of the Kamada-Kawai algorithm, the same algorithm as described above was applied and, thus, the areas were split in two sets based on the optimal partition resulting in the highest topological symmetry.

Since the algorithm will always result in a division of the areas, the frequency of the assignments of the areas of the original cortico-cortical networks was compared to the frequency of the assignments of the areas obtained from null networks that were matched for degree, number of nodes and connections with the original networks (Bezgin et al., 2014). We run 100 null network instantiations and the distribution of the null frequency of the assignments of areas was compared with the distribution obtained for the original networks. Difference between the two distributions was assessed with the

statistical energy test, a non-parametric statistic for two-sample comparisons (Aslan & Zech, 2005) (<https://github.com/brian-lau/multidist/blob/master/minetest.m>) and statistical significance was assessed with permutation tests.

## 2.6. Physical embedding of the dual connectional trends

The theory of the dual origin of the cerebral cortex postulates that cortical areas have a paleocortical or archicortical affiliation, that is, they constitute successive waves of progressive laminar differentiation emanating from the paleocortex or archicortex (Abbie, 1940, 1942; Pandya et al., 2015; Sanides, 1962). Therefore, we examined the dual connectional trends derived from the previous step in relation to a spatial map of the cerebral cortex that measures the physical distance from the archicortex and paleocortex. For each cortical area, the average physical distance from the archicortex and paleocortex was computed and a winner-takes-all map was created by assigning an affiliation to each cortical area based on the moiety (archicortex or paleocortex) that was spatially closer to the cortical area. The affiliation of each area to a connectional trend was used to assess if the dual connectional trends are different with respect to their physical distance from the archicortex and paleocortex. Differences were assessed with the statistical energy test and statistical significance was assessed with permutation tests. The aforementioned distance maps were computed for the species for which 3D surfaces and parcellations were available, that is, the macaque monkey, mouse and rat.

## 2.7. Transcriptome analysis

Gene expression data from the Allen Brain Atlas (ABA) derived from *in situ* hybridization from the adult C57BL/6J male mouse at age P56 (Lein et al., 2007) were extracted from the Brain Gene Expression Analysis Toolbox (<http://www.brainarchitecture.org/allen-atlas-brain-toolbox>) (Grange, Bohland, Hawrylycz, & Mitra, 2012). These data were used to examine the molecular differences of the uncovered dual connectional trends in the mouse cortex. The toolbox contains the gene expression values of 4005 genes that are part of the coronal dataset of the ABA. This dataset was downloaded from the API of the Allen Institute (<http://help.brain-map.org/display/mousebrain/API>). The so-called expression energy was used as the quantitative metric of the expression of each gene (Fulcher & Fornito, 2016; Lein et al., 2007). The Allen Reference Atlas (ARA) was used in order to summarize gene expression values in an area-wise manner. The average values for each area were computed by taking into account available measurements falling within each area. For each gene, the gene expression values across areas were transformed with a sigmoid function (Fulcher & Fornito, 2016) in order to render comparisons across genes feasible and reduce the effect of outlier values arising from artefacts in the high-throughput pipeline (e.g., dust and errors in the segmentation algorithm, reduced permeability of the probes). The procedure resulted in a  $38 \times 3787$  matrix of normalized gene expression values of 38 cortical areas for each hemisphere. For the main analysis, we analyzed the right hemisphere data for congruency with the mouse

connectional dataset, and used the transcriptome data from the left hemisphere as a control/robustness analysis.

The cortical area by gene expression matrix was decomposed with principal component analysis (PCA) in order to reveal the major axes of organization of the cerebral cortex across which the largest amounts of variance of gene expression manifest. These axes of organization were compared to the division that corresponds to the dual connectional trends by examining the separability of the two connectional streams across the dimensions defined by the principal components (PCs). The statistical energy test and permutation tests were used to assess the separability of the dual connectional trends in each PC separately. In addition, we carried out a targeted analysis that focused on genes coding for families of proteins functioning as morphogens that exhibit a graded expression across the developing pallium (e.g., O'Leary et al., 2007; Tiberi, Vanderhaeghen, & van den Ameele, 2012). Differences in the expression of such genes in the two trends were assessed with the statistical energy test and permutation tests.

## 2.8. Computational modeling of neurogenetic gradients and connectivity formation

Heterochronicity in the development of the brain, that is, temporally distinct neurodevelopmental events, appears crucial for the establishment of intricate wiring patterns observed in the adult brain (Bayer & Altman, 1987; Goulas, Betzel, & Hilgetag, 2018; Kaiser, 2017; Kaiser & Hilgetag, 2007). We employed a modeling approach in order to address the feasibility of a mechanism based on heterochronous development to generate the symmetric connectional topology, that is, the dual connectional trends, observed in the empirical cortical connectomes. Specifically, based on empirical observations (Smart, 1984), we simulated spatially ordered neurodevelopmental gradients of release and accumulation of neuronal populations in the pallium in distinct developmental time windows. Pillars of the current approach are the studies of Kaiser and Hilgetag (2007) and Nisbach and Kaiser (2007).

A square 2D synthetic cortical sheet was used, with each pixel representing a unit surface of the cortical plate hosting up to  $N$  neurons. Each pixel in this artificial sheet is assigned a time window that specifies at each time point  $t$  during the synthetic developmental process the probability of  $n$  neurons migrating at the cortical plate location defined by the pixel. The peak of the migration probability of each time window of each pixel is linearly related to the minimum physical distance of the pixel from the roots of the neurodevelopmental gradients. Thus, population of the synthetic sheet proceeded in an heterochronous and spatially ordered manner with two origins from which the neurodevelopmental gradients spread as co-centric rings. The two origins were randomly placed in the synthetic cortical sheet. The initial number of neurons to populate the cortical sheet was set to 100. At each developmental time step, the number of neurons that can populate the cortical sheet increased exponentially, as empirical data indicate (Caviness, Takahashi, & Nowakowski, 1995), according to the formula  $n = n_{\text{initial}} * (1 + r)^t$ , where  $n_{\text{initial}}$  is the initial number of neurons,  $r$  the rate of neuronal increase at each time point and  $t$  the developmental time point of the

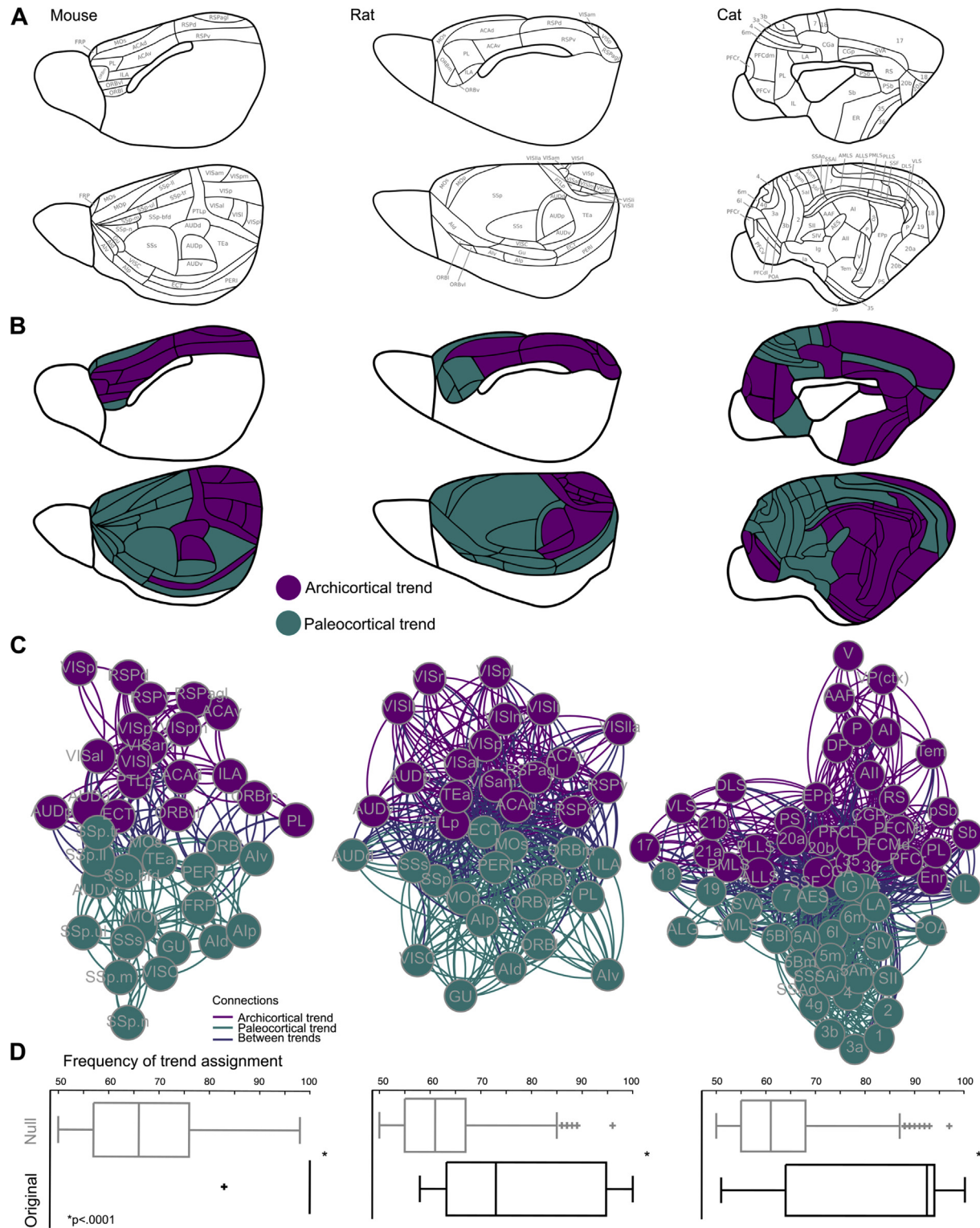


**Fig. 3 – Dual connectional trends in the mouse, rat and cat cerebral cortex.** A. Mouse map based on Dong (2008). Rat map based on Swanson (2004). Cat map from Scannell et al. (1995). B. Maps showing the dual connectional trends. Areas are color-coded based on their more frequent assignment to each trend. The two trends are named as paleocortical or archicortical based on the areas that they contain and their distance from the paleocortex and archicortex (see Fig. 4). Specifically, archicortical areas, such as the areas of the retrosplenial cortex, as dictated by the dual origin framework (Pandya et al., 2015), are used to name the division that they belong to. The same holds for the paleocortical areas, such as the areas of the insular cortex. B. 2D layout corresponds to a Fruchterman-Reingold force-directed graph drawing. Areas that are proximally located in this 2D space are topologically more similar than remote areas. C. The assignment of areas to the two topologically symmetric structures, defining the dual connectional trends, is statistically significantly more stable compared to the assignments derived from a null model with

simulations. The rate of neuronal release was set to .1. When neurons were placed in the synthetic cortex, they developed connections by extending an axon as a straight line. The direction for growing an axon was sampled from a uniform distribution and a connection was formed when an axon hit another neuron in the synthetic sheet (Kaiser, Hilgetag, & van Ooyen, 2009). Simulations unfolded across 25 time points. In total, 10 synthetic cortical sheets were simulated.

The synthetic cortical sheet was randomly parcellated into “cortical areas” with a Voronoi tessellation. The number of the cortical areas was based on the empirical parcellation of the cortex of a species. These areas served as the basis of assembling a cortico-cortical area-by-area connectivity matrix. The synthetic connectivity matrix was thresholded at the density dictated by the empirical connectivity matrix by removing the weakest connections. The synthetic cortico-cortical matrix was subject to the same algorithm that was used for the empirical data, thus splitting the areas in two topologically symmetric parts, resulting in the dual connectional trends.

Since the algorithm will always split the areas in two parts, the quality of the split was assessed by computing the stability of the assignments of the areas in the two splits in the same way as for the empirical data. This quantitative metric allowed us to assess if heterochrony is an essential component of the suggested neurodevelopmental mechanism for the generation of the observed dual connectional trends in the cortex. To this end, the simulations were run by using the exact same synthetic cortical sheet generated in the heterochronous simulations, but now all neurons were placed simultaneously in the sheet and formation of connections took place with all the neurons simultaneously present in the cortical sheet (tautochronous development). Stability of the assignments of the areas in two splits in the tautochronous development scenario was compared to the stability of the assignments in the heterochronous development scenario.

### 3. Results

#### 3.1. Dual connectional trends in the mammalian cortex: topologically symmetric structures

Results from previous analysis applied to the prefrontal-auditory system (Bezgin et al., 2014) (Fig. 2A) are congruent with the predictions of the dual origin framework (Pandya et al., 2015) (Fig. 2B). The results from the whole-cortex connectivity dataset for the macaque monkey revealed a dual architecture for the totality of the macaque monkey cortex, across functional systems and lobes, with one trend covering the cingulate cortex and the dorsal parts of the frontal and parietal cortex, and the other trend covering the ventral parts of the frontal and parietal cortex (Fig. 2C). The consistency of assignment of areas in the two trends was statistically significantly higher than the trend assignments of matched null networks ( $p < .0001$ , permutation test) (Fig. 2C). The

topological similarity of the dual trends and their spatial extent across the monkey cerebral cortex are depicted in (Fig. 2C). Thus, the results in the macaque monkey revealed a congruency with the predictions of the dual origin framework (Pandya & Yeterian, 1985; Pandya et al., 2015) (Fig. 2B and C). A notable exception concerns visual areas V1 and V2 and somatosensory area 2. The medial surface of areas V1 and V2 presumably belongs to the archicortical trend, while the lateral surface to the paleocortical trend (Pandya et al., 1988). With respect to area 2, the ventral part should belong to the paleocortical trend, whereas the dorsal part to the archicortical trend (Pandya et al., 2015). These discrepancies arise due to the parcellation used to assemble the connectional data (Markov et al., 2014), which does not distinguish between a dorsal and ventral area 2 or a medial and lateral surface of V1 and V2.

A topologically symmetric structure, defining the dual connectional trends, was detected in all mammalian species (Fig. 3). The algorithm partitioned the cortical areas in spatially contiguous dual trends, with one set of areas traced back to the less eulaminated insular cortex, hence, termed as paleocortical trend, while the other set of areas can be traced back to the less eulaminated cingulate and retrosplenial cortex, hence, termed as archicortical trend (Fig. 3A and B). The topological similarity of the cortical connectomes of all the species, defining the dual trends, is depicted in (Fig. 3C). The area-by-area frequency of trend assignments for all species is enlisted in (Table S1). The consistency of assignment of areas in the two streams was statistically significantly higher than the assignments of matched null networks for all species (Fig. 3D). The additional dataset for the mouse cortex (Zing et al., 2014), revealed congruent results with the data from (Oh et al., 2014) (Fig. S1). It is noteworthy that the inclusion of the piriform, lateral entorhinal cortex and the dorsal part of the subiculum, as available in the Zing et al. (2014) dataset, led to the assignment of the piriform and lateral entorhinal cortex to the paleocortical trend, while the dorsal subiculum was assigned to the archicortical trend (Fig. S1). These results are in line with the dual origin framework, since the piriform cortex is the primordial formation for the paleocortical stream and the hippocampus the primordial formation for the archicortical stream (Pandya et al., 2015) (Fig. 1). It is noteworthy that the dual connectional architecture corresponds to pallial divisions of the mouse (Pattabiraman et al., 2014). Specifically, the archicortical trend, that was detected on a connectional basis, encompasses parts of the medial and dorsomedial pallium, namely, the subiculum, and cingulate, retrosplenial and prelimbic cortical areas (Fig. 3 and Fig. S1). The paleocortical trend, that was detected on a connectional basis, encompasses parts of the ventral and lateral pallium, namely, the piriform cortex, along with insular and perirhinal cortical areas (Fig. 3 and Fig. S1). The dorsal pallium seems subject to two spheres of influence, namely the paleocortical influence that dominates the motor and somatosensory areas, while the visual areas are

dominated by the archicortical formation. Notably, the aforementioned pallial divisions are influenced by distinct patterning centers and are dominated from distinct neurogenetic gradients with distinct origins (e.g., Aboitiz & Montiel, 2015; Smart, 1984; Tiberi et al., 2012).

The affiliation of the connectional trends to the archicortical and paleocortical formations is also reflected in the spatial maps of the cortex that measure the physical distance of each area from the archicortex and paleocortex (Fig. 4A). The two connectional trends were primarily spatially affiliated with either the archicortical or the paleocortical formations (statistical energy test,  $p < .05$ , Bonferroni corrected, permutation tests) (Fig. 4B). Only the paleocortical trend in the macaque monkey failed to exhibit statistically significant differences (Fig. 4B). Hence, the dual connectional trends in all investigated mammalian species are aligned with spatial spheres of influence of the archicortical and paleocortical formations, the later reminiscent of geometric antipodal formations in the cortical sheet.

In sum, in all examined species, a connectivity-based division of cortical areas in topologically symmetric structures defined the dual connectional trends. This division aligns well with the predictions and prior knowledge from the dual origin framework. The dual connectional trends are spatially closer to either the archicortical or paleocortical formation and form spatial constellations reminiscent of geometric antipodal formations across the cortical sheet. Lastly, the dual trends encompass different subdivisions of the developing pallium, suggesting distinct origins of these connectional structures during the ontogeny of the pallium.

### 3.2. Dual connectional architecture and cortical transcriptome

For one of the mammalian species, that is, the mouse, a detailed whole-cortex transcriptome is available. Thus, we proceeded to the comparison of the whole-cortex transcriptome with the dual connectional trends. The PCA decomposition of the cortical transcriptome unraveled major axes of its organization, namely dimensions explaining the maximum amount of gene expression variance across the cortical sheet. The connectivity-based division of the cortex in two trends corresponded to the 4th PC, explaining 11.6% of the transcriptome variance (Fig. 5A). The separation of cortical areas based on their dual connectional trend affiliation was only observed across the 4th PC (statistical energy test,  $p < .05$ , Bonferroni corrected, permutation tests) (Fig. 5A). It is noteworthy that the 4th PC is the last PC explaining a substantial amount of variance after a decrease, the so-called “elbow”, in the variance explained by the PCs was observed (Fig. 5A). Separation of cortical areas belonging to the two trends along PC4 was also visually evident when PC4 was plotted against PCs 1–3 (Fig. 5B). It should be noted that the PCA decomposition is blind to the grouping of the cortical areas in the two trends. Therefore, the arrangement dictated by PC4 is a natural axis of organization of the mouse cortical transcriptome that aligns with the dual connectional trends (Fig. 5C).

A targeted analysis focused on genes coding for families of proteins functioning as morphogens. These morphogens have a graded expression across the pallium (e.g., O’Leary

et al., 2007; Tiberi et al., 2012). Significant differences were detected between the gene expression profiles of the two connectionally defined trends (Fig. 6). Specifically, expression of genes coding for bone morphogenetic proteins (BMP) differed significantly between the two trends ( $p < .05$  uncorrected). Note that all differences reported in this section are assessed with the statistical energy test and statistical significance was assessed with permutation tests. Iteration of all combinations of the BMPs revealed that *Bmp5* led to the highest separation between the two streams ( $p < .05$ , Bonferroni corrected) (Fig. 6A). Higher average expression of BMP was observed for the archicortical trend (Fig. 6A). Expression of genes coding for ephrins (EPH) did not differ significantly between the two trends ( $p > .1$ ). Iteration of all combinations of the EPHs revealed that *Epha1* and *Epha8* led to a small difference between the two trends ( $p < .05$ , uncorrected), with the archicortical trend exhibiting higher expression (Fig. 6B). Expression of genes coding for proto-oncogene proteins (WNT) did not differ significantly between the two trends ( $p > .1$ ). Iteration of all combinations of the WNTs revealed that *Wnt8a* led to a small difference between the two trends ( $p < .05$ , uncorrected), with the archicortical trend exhibiting higher values (Fig. 6C). Expression of genes coding for early growth factor proteins (EGR) differed between the two trends ( $p < .05$ , Bonferroni corrected). Iteration of all combinations of the EGRs revealed that *Egr3* led to the highest significant difference between the two trends ( $p < .05$ , Bonferroni corrected), with the archicortical trend exhibiting the highest values (Fig. 6D). Expression of genes coding for fibroblast growth factors (FGF) differed significantly between the two trends ( $p < .05$ , Bonferroni corrected). Iteration of all combinations of the FGFs revealed that *Fgf13* led to the highest significant difference between the two trends ( $p < .05$ , Bonferroni corrected), with the paleocortical trend exhibiting the highest values (Fig. 6E). Lastly, both expression of insulin growth factor 2 (*Igf2*) and Sonic hedgehog (SHH) differed between the connectional trends (*Igf2*,  $p < .05$ , Bonferroni corrected, SHH,  $p < .05$ , uncorrected), with the paleocortical trend exhibiting the highest values (Fig. 6E). We should note that the exact same analysis, but using the left hemisphere data, led to consistent results (Fig. S2). A notable exception was the gene expression for *Igf2* and SHH, which did not reach statistical significance for the left hemisphere. Only consistent results in both the left and right hemispheres were taken into account when summarizing the results of the relation of gene expression and the dual trends in the mouse cortex. We should note that the aforementioned differences of gene expression between the two trends do not preclude the common expression of other genes.

In sum, the archicortical trend exhibits higher expression than the paleocortical trend for bone morphogenetic proteins (BMP5), ephrins (*Epha1*, *Epha8*), proto-oncogene proteins (Wnta8a) and early growth factor proteins (Egr3). The paleocortical trend exhibits higher expression than the archicortical trend for fibroblast growth factors, particularly for *Fgf13*. These results demonstrate the presence of a trace of the expression of different morphogenetic gradients in the adult mouse cortex that differentially characterize the dual trends.

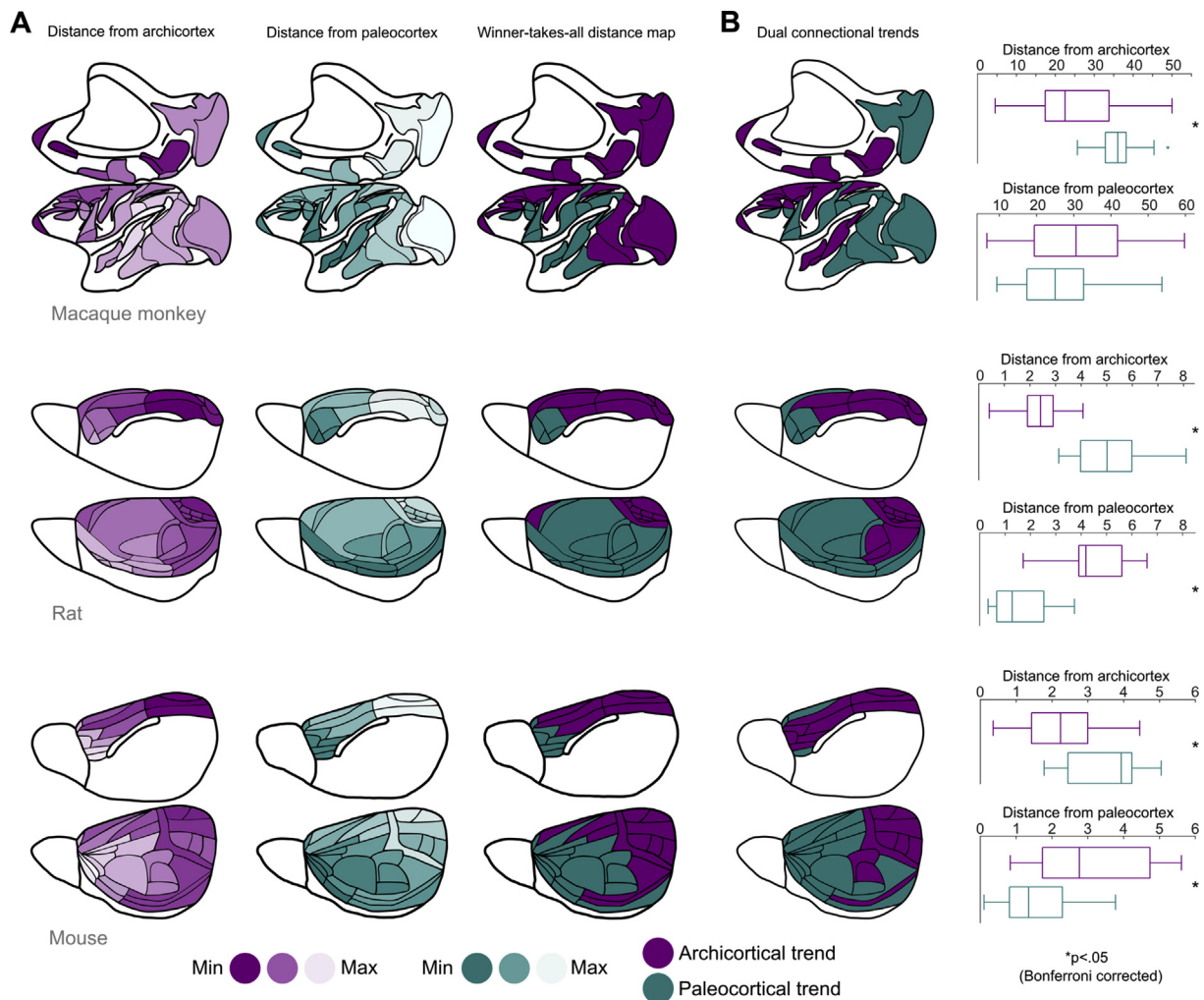


**Fig. 4 – Distance maps from the archicortical and paleocortical formations in relation to the dual connectional trends.** A. Spatial distance of cortical areas from the paleocortex and archicortex depicted for the macaque monkey, rat and mouse. The winner-takes-all maps depict the cortical areas that are spatially closer to either the paleocortex or archicortex. Note that the winner-takes-all maps match very closely the dual connectional trends maps (panel B). B. Areas that belong to the archicortical (paleocortical) trend, defined on a connectional basis, are statistically significantly closer to the archicortex (paleocortex) (statistical energy test). The two trends are spatially arranged in a way that is reminiscent of geometric antipodal structures across the cortical sheet.

Therefore, different morphogenetic gradients might influence the neurodevelopmental trajectory of the two trends during the development of the pallium. It is plausible that a mechanism for the formation of the dual connectional trends in the adult cortex might be rooted in development and, as we elaborate below, such mechanism is supported by computational modeling.

### 3.3. Neurodevelopmental gradients and connectivity formation result in the dual connectional trends

The simulation of neurodevelopmental gradients emanating from two sources, the subsequent stochastic connectivity formation between the neuronal populations and the application of

the algorithm for the detection of the dual symmetric topology to the resulting synthetic connectome (Fig. 7A,B), led to two spatially contiguous divisions of the synthetic cortical sheet (Fig. 7C). The division seems to have two spheres of influence, that is, the two sources from which the neurodevelopmental gradients propagated as co-centric rings (marked with grey circles in Fig. 7C). The comparison of the stability of the assignment of cortical areas into two trends from simulations characterized by heterochronous development with the stability of assignments from simulations characterized by a tautochronous development, revealed a higher stability of the assignment of areas in two trends for the heterochronous simulations when compared to the tautochronous simulations (Fig. 7C) (statistical energy test,  $p < .0001$ , permutation test).

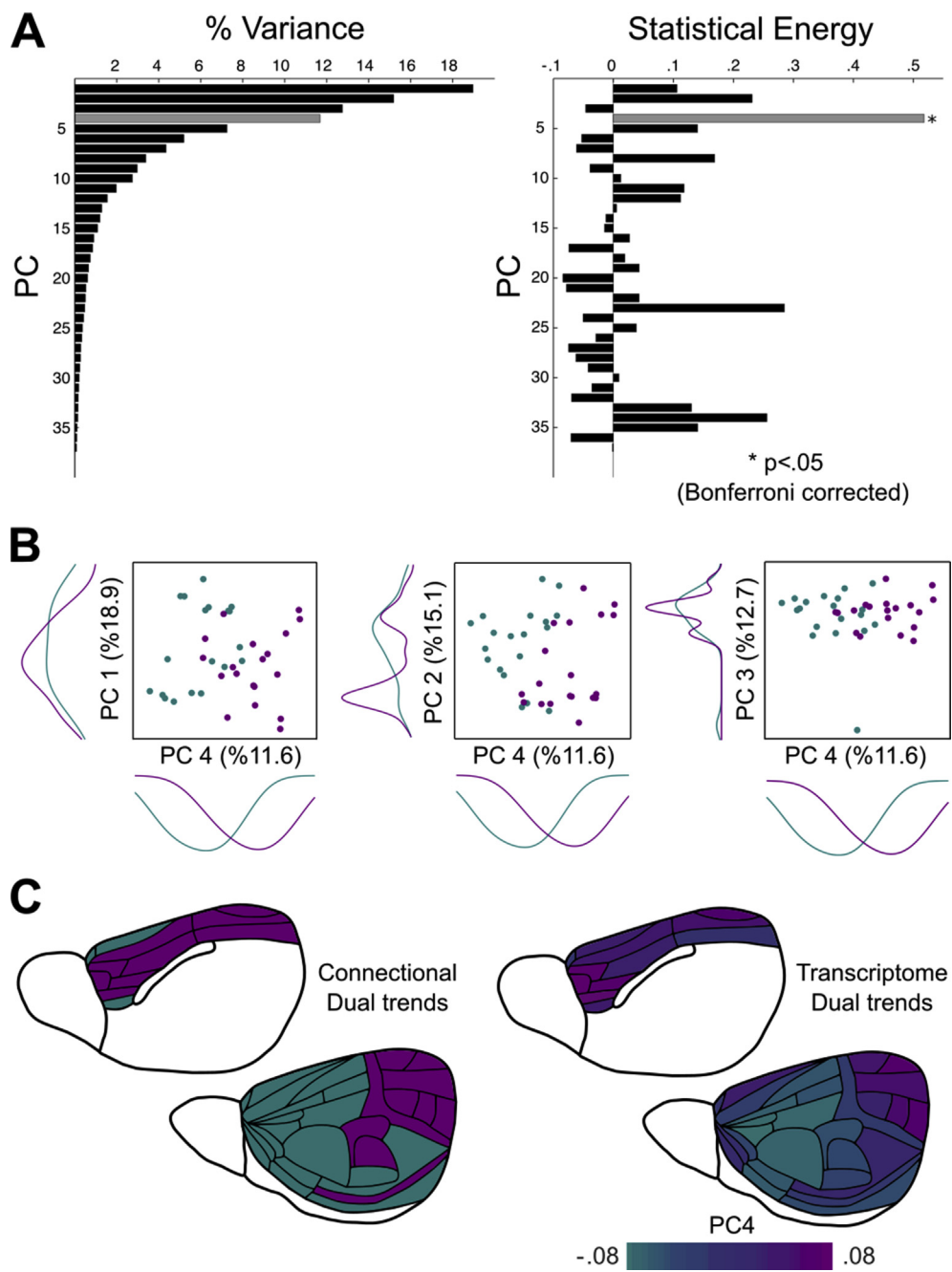


**Fig. 5 – Dual connectional trends and transcriptome architecture of the cortex.** A. Variance explained by each PC and separation of the dual connectional trends across each PC. The dual connectional trends are separated across PC4 (grey color). B. Scatter plots demonstrating the separation of the dual connectional trends across PC4 when plotted against PC1-3. C. Cortical rendering of the arrangement of cortical areas across PC4. Each color corresponds to the coordinate of each area in PC4. Purple colors correspond to areas increasingly affiliated with the archicortex, whereas petrol green colors indicate areas with increased affiliation with the paleocortex. Note the striking natural arrangement of areas across PC4, based on gene expression, that tightly corresponds with the connectivity-defined dual trends.

In sum, the modeling results dictate the following instructive points. First, a neurodevelopmental mechanism based on the heterochronous population of the synthetic cortex with neurons and the subsequent stochastic connectivity formation between the neuronal populations is

sufficient to generate a spatially contiguous division based on topological symmetry, that is, dual connectional trends. Second, the heterochronous population of the synthetic brain is a necessary component of the underlying neurodevelopmental mechanism.

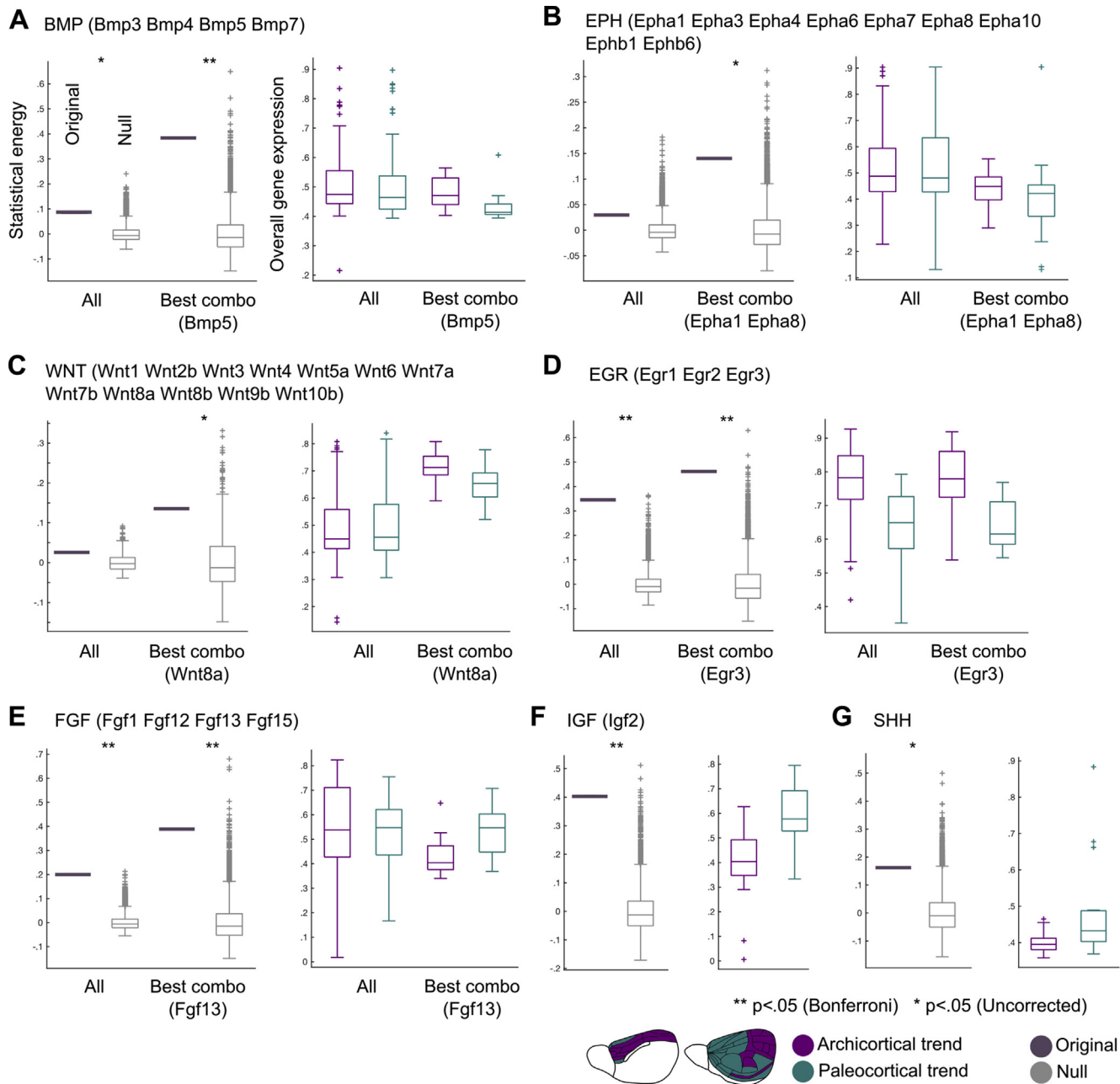


**Fig. 6 – The dual connectional trends exhibit differences in the levels of expression of genes coding for morphogens.** Differences between the two trends are tested for genes coding for A. Bone morphogenetic factors (BMP) B. Ephrins (EPH) C. proto-oncogene proteins (Wnts) D. Early growth response (EGR) E. Fibroblast growth factors (FGF) F. Insulin growth factor (IGF) G. Sonic hedgehog (SHH). These differences dictate that the ontogeny of the dual connectional trends is bound to different patterning centers in the developing pallium and under the influence of different morphogens the trace of which is reflected in the adult cortex. Note that the summary of the overall gene expression for each trend, in cases of summaries involving the expression of more than one gene, does not preserve the multidimensional space where the differences between the two trends were actually tested. Differences were assessed with the statistical energy test.

#### 4. Discussion

Like the rings of a tree, the cerebral cortex consists of rings of progressive laminar differentiation emanating from the paleocortical and archicortical formations. This is the basic premise of the dual origin of the cerebral cortex, a theory with multiple reincarnations (Abbie, 1940, 1942; Dart, 1934; Pandya

et al., 2015; Sanides, 1962, 1970; Shellshear, 1929). This theory is reinstated through our results in the age of connectomics and high throughput transcriptome mapping of the cerebral cortex. Our results dictate that the duality of the cortex is reflected at the connectional, transcriptional and spatial dimension of the cerebral cortex of mammals, possibly the result of two neurogenetic gradients in the developing pallium

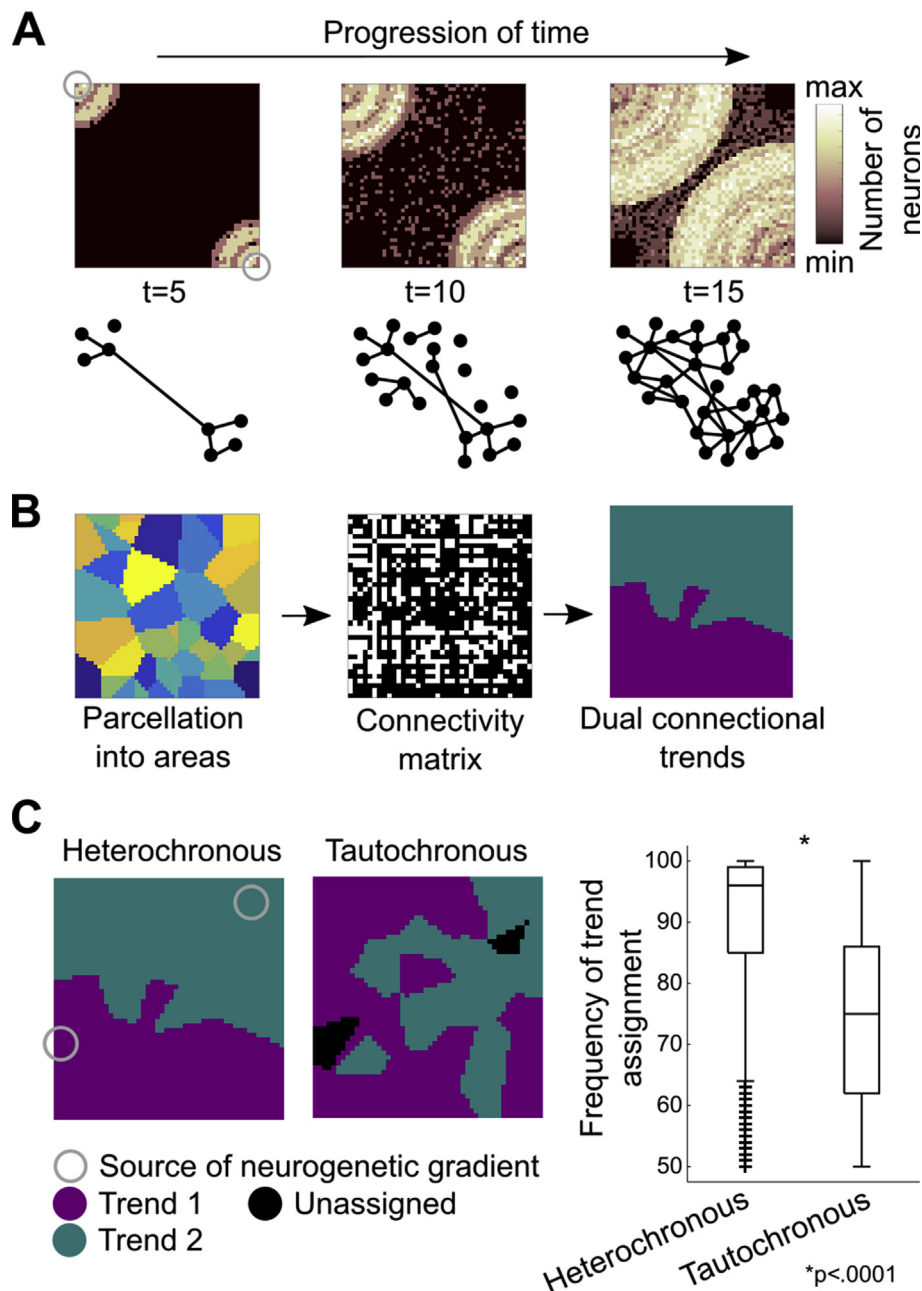


**Fig. 7 – Computational modeling of neurodevelopmental gradients and connectivity formation.** A. Neurodevelopmental gradients were simulated in a synthetic cortical sheet and connectivity was established with random growth of axons. B. The synthetic cortex is parcellated into “cortical areas” and a synthetic cortico-cortical matrix is obtained. C. The application of the dual connectional trend algorithm to the synthetic connectome indicates that the most stable dual structure emerges when the simulations are based on heterochronous development. Tautochronous development leads to more unstable assignments of areas to the two connectional trends. Thus, heterochronous development and stochastic connectivity formation can constitute components of a mechanism for the ontogeny of the dual connectional trends. Note that in the depicted example, the synthetic cortical sheet was parcellated in a number of areas that matched the number of areas in the mouse cortex and the synthetic connectivity matrix was matched with the density of the empirical mouse connectome. Similar results were obtained for parcellations and density thresholding corresponding to the empirical connectomes of the other species.

(Fig. 8). Moreover, the two trends reflect different pallial divisions (Fig. 8). Hence, our results demonstrate that the duality of the cortex is a major axis of organization across which a plethora of multimodal data within and across species can be

understood. Moreover, we have offered a basic, putative neurodevelopmental mechanism for this dual architecture, thus increasing the explanatory depth of the dual nature of the cerebral cortex.

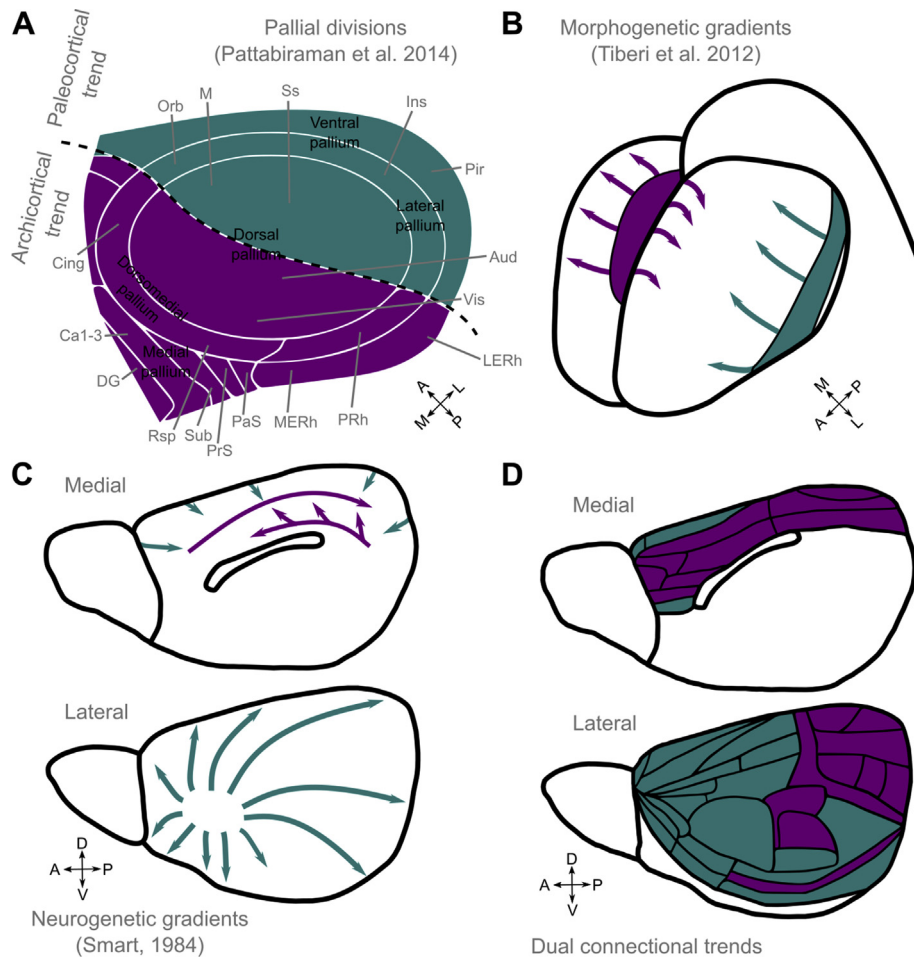


**Fig. 8 – Dual connectional trends reflected in pallial divisions, patterning centers and neurogenetic gradients.** A. Dual connectional trends encompass distinct pallial divisions. The archicortical trend encompasses the medial, dorsomedial and half of the dorsal pallium. The paleocortical trend encompasses the ventral, lateral and half of the dorsal pallium. Note that only main divisions are named. B. Patterning centers of morphogens expressed in a graded fashion in the developing pallium. The two origins are the cortical hem (purple), presumably related to the archicortical trend, and the cortical “anti-hem” (petrol green), presumably affiliated with the paleocortical trend. C. Neurogenetic gradients in the developing mouse pallium. Arrows indicate an early to late heterochronous neurogenesis. Note the different loci of neurogenetic gradients populating the developing pallium, presumably underlying the ontogeny of the dual connectional trends. D. Dual connectional trends in the mouse defined by the present analysis. Note the correspondence of the dual trends with the divisions illustrated in panels A–C. Abbreviations: Aud: Auditory; CA1-3: CA fields 1–3; Cing: Cingulate; DG: Dentate gyrus; Ins: Insula; LERh: lateral entorhinal; MERh: medial entorhinal; M: Motor; Orb: Orbital; Pir: Piriform; Prs: Presubiculum; PaS: Parasubiculum; PRh: Perirhinal; Rsp: Retrosplenial cortex; Ss: Supplementary somatosensory; Sub: Subiculum; Vis: Visual. A: Anterior; P: Posterior; D: Dorsal; V: Ventral; M: Medial; L: Lateral.

#### 4.1. The dual origin of the cerebral cortex is reflected in the connectional architecture of different mammalian species

Uncovering organizational principles of the cerebral cortex is essential for understanding the complexity of the various levels of cortical architecture. The dual origin of the cortex is such an organizational principle and offers a framework for systematizing dispersed observations, at the cyto- and myeloarchitectonic and connectional levels (Abbie, 1940, 1942; Sanides, 1962, 1970; Sanides & Hoffmann, 1969; Pandya & Yeterian, 1985; Pandya et al., 2015). Conceiving the dual connectional trends as a division into topologically symmetric

structures (Bezgin et al., 2014), we quantitatively demonstrated the presence of dual connectional trends in the macaque monkey at the global, whole-cortex level (Fig. 2B,C). This division is in line with prior qualitative observations based on the cyto-, myeloarchitecture and connectional architecture of the macaque monkey (Pandya et al., 2015; Sanides, 1970). For instance, the two connectional streams fuse in the lateral surface, with the principal sulcus and the intraparietal sulcus as macroscopic borders (Fig. 2B,C). Hence, the usual division of systems of the macaque monkey cortex in a dorsal and ventral compartment, for instance, the dorsal and ventral prefrontal cortex, a division based on the principal sulcus, has its basis on the dual connectional architecture,

that now presents itself as a quantifiable topologically symmetric connectional architecture.

The quantification of the dual connectional trends in the mouse, rat and cat cortical connectomes, revealed the presence of such trends in all these species (Fig. 3). This division splits the areas in two spheres of influence, one paleocortical, encompassing areas like the insula, pyriform cortex (paleocortical stream) and one archicortical, encompassing the retrosplenial and cingulate areas (archicortical stream) (Fig. 3). Furthermore, each dual connectional trend is spatially closer to either the paleocortex or archicortex and the trends are spatially arranged in such a fashion that is reminiscent of antipodal geometric structures across the cortical sheet (Fig. 4).

The current results allow dispersed observations to be unified within the coherent framework of dual cortical organization. For instance, elaborate connectional data of the mouse cortex (Zingg et al., 2014) demonstrate the presence of two large-scale networks, the so-called medial and lateral networks. In light of the current results, these networks are parts of the archicortical and paleocortical streams (Fig. S1). Thus, the current results allow the transition from pure topological network divisions (medial, lateral, etc.) to the unifying dual origin framework, wherein such networks are understood as an organization scheme that spans different species, and encompasses the cyto-, myeloarchitectonic and transcriptional dimensions of cortical organization, with different correspondence to different pallial divisions and, plausibly, different neurogenetic origins (Fig. 8).

#### **4.2. The dual connectional architecture is an axis of organization of the cortical transcriptome and reflects patterning centers in the developing pallium**

Decomposition of the cortical transcriptome of the mouse in its major organizational axes revealed that a substantial amount of variance of gene expression across the cortical sheet is organized around the axis formed by the arrangement of cortical areas in dual connectional trends (Fig. 5). Thus, we revealed the molecular basis of the dual connectional trends, highlighting the dual origin of the cortex as a dimension to be significantly related to a major axis of transcriptome organization of the mammalian cortex, therefore contributing to a growing literature that seeks to uncover transcriptome organizational principles in mammals (Bernard et al., 2012; Hawrylycz et al., 2012).

The dual connectional trends exhibit differences in gene expression coding for proteins that function as morphogens that control the patterning and neurogenesis in the cerebral cortex (e.g., Borello & Pierani, 2010; Tiberi et al., 2012) (Figs. 6 and 8). In the developing pallium, two major patterning centers exist, that is, the hem, expressing BMP and WNT, and the “anti-hem”, located at the pallial/subpallial boundary and expressing FGF (Borello & Pierani, 2010; O’Leary et al., 2007; Tiberi et al., 2012). The dual connectional trends differ in the expression of these morphogens. Specifically, the archicortical trend expresses more BNP, WNT, EGR and EPH, whereas the paleocortical stream expresses more FGF (Fig. 6, Fig. S2). Therefore, the two trends can be conceived as spheres of influence of two main patterning centers in the developing

pallium, thus offering a plausible explanatory framework for the ontogeny of the dual connectional trends (Fig. 8).

#### **4.3. Heterochronous neurodevelopmental gradients offer a mechanistic explanation of the ontogeny of the dual connectional trends**

The emergence of the dual connectional trends might be rooted in two patterning centers in the developing pallium, resulting in two opposing neurogenetic gradients, as empirical evidence dictates (Fig. 8). Simulation of neurodevelopmental gradients and connectivity formation in a synthetic cortical sheet demonstrates the feasibility of such mechanism (Fig. 7). The simulations indicate that the dual connectional trends can emerge from two sources of heterochronous neurodevelopmental gradients. Importantly, the heterochronicity in development and subsequent connectivity formation is necessary for the consistent partition of cortical areas in a stable and spatially contiguous dual structure (Fig. 7). In sum, heterochronous development and connectivity formation constitutes a realistic mechanism for the ontogeny of the dual connectional trends that are observed in the adult cortex.

From a broader standpoint, the computational modeling results demonstrate the importance of heterochronicity in development and connectivity formation. Empirical evidence in rats demonstrate that orderly topographic connections between the olfactory bulb and primary olfactory cortex are dictated by the temporal proximity of the interconnected neuronal populations during neurogenesis (Bayer & Altman, 1987). Computational modeling has also highlighted the importance of distinct time-windows in development for the formation of tightly interconnected sets of areas, the so-called modules (Kaiser & Hilgetag, 2007), as well as the faithful reconstruction of inter-regional wiring principles (Goulas, Betzel et al., 2018). Our modeling results exemplify once more the importance of heterochronous neurodevelopmental events in the formation of intricate connectional topologies in the adult cerebral cortex.

#### **4.4. Functional and behavioral implications**

Early architects of the dual origin theory have emphasized the functional and behavioral significance of the dual structure of the cerebral cortex. Specifically, a broad distinction was proposed, with the paleocortical trend affiliated with object identification (“what” stream) and the archicortical stream affiliated with object localization (“where” stream) (Pandya & Yeterian, 1990). Such conceptualization of the two trends also resonates well with recent suggestions postulating that the isocortex is shaped by behavioral adaptations centered around olfaction- and navigation-related functions, associated with the paleo- and archicortex, respectively (Aboitiz & Montiel, 2015). The dual origin of the cortex also provides a framework for understanding clinical cases involving behavioral deficits (Giaccio, 2006). For instance, schizophrenia can be conceptualized and understood in terms of an imbalance and lack of integration of the functions related to the paleo- and archicortical trends, with negative symptoms mostly associated with disturbances of the archicortical trend and positive symptoms with the paleocortical trend (Giaccio,

2006). Moreover, brain lesions, a classic method for assessing brain-behavior relations, can also be understood within the dual origin framework, since lesions in different trends, for instance, the dorsal or ventral parts of the prefrontal cortex, seem to have different behavioral impact (Giaccio, 2006). Therefore, despite that more quantitative examination is needed, the duality of the cortex offers a framework wherein not only structural, but also functional and behavioral aspects of cortical organization, can be understood. Applying the current methods to the human cerebral cortex in conjunction with functional mapping studies involving a plethora of cognitive and behavioral domains will offer a more concrete view of the duality of the cortex and its association with cognition and behavior.

#### 4.5. The duality of the cortex as one of the major natural axes of the cerebral cortex

Our results demonstrate that the duality of the cortex is an organizational axis of the cerebral cortex reflected in its transcriptional, connectional and geometric dimensions. Therefore, this duality can be conceived as a natural axis of cortical organization.

Classic and more recent studies of the mammalian cortex have sought to uncover the natural dimensions of systematic variations of cortical features (“Main directions of differentiation”–*Hauptdifferenzierungsrichtungen*–Brockhaus, 1940), including myeloarchitecture (Brockhaus, 1940; Sanides, 1962; Sanides & Hoffmann, 1969; Huntenburg et al., 2017; Burt et al., 2018; Fulcher, Murray, Zerbi, & Wang, 2019), cytoarchitecture (von Bonin & Bailey, 1961; Sanides, 1962; Pandya & Yeterian, 1985; García-Cabezas, Zikopoulos, & Barbas, 2019), laminar origin of connections (Barbas, 1986; Goulas, Zilles, & Hilgetag, 2018; García-Cabezas et al., 2019), functional connectivity (Margulies et al., 2016) and gene expression (Burt et al., 2018; Fulcher et al., 2019). Such studies indicate that the transition from cortical areas with less to more laminar differentiation constitutes another major axis of cortical organization across which cortical features systematically vary (Margulies et al., 2016; Burt et al., 2018; Goulas, Zilles et al., 2018; Fulcher et al., 2019) and that such changes have functional and behavioral ramifications (Margulies et al., 2016; Huntenburg et al., 2017). Three further observations from our results are noteworthy in that respect. First, the major axes of variance of the mouse transcriptome also includes a less to more differentiation axis (in broad terms, cingulate and insular cortex to sensorimotor cortex) (PC1 in Fig. 5 and Fig. S3). Second, PC2 seems to correspond to the anterior-posterior axis of the brain, an observation that resonates well with previous suggestions of cortical organization (Charvet & Finlay, 2014). Third, the gene expression variance explained by each PC is rather balanced between the first 4 PCs, that is, PC1 explains approximately 18%, PC2 15%, PC3 12% and PC4 11% (Fig. 5), indicating that a multiplicity of natural cortical dimensions exists.

In sum, the current results, in conjunction with literature that spans several decades, indicate that while the dual trends constitute an organizational principle of the cortex, such organization should be viewed as one important manifestation

of the multiple natural axes of the cerebral cortex. Elucidating the ontogeny and relations between these natural axes and how they relate to behavioral and cognitive aspects, as well as how they vary across species, will offer a unifying framework of cortical organization with unprecedented explanatory and predictive power.

#### 4.6. Limitations and future directions

We should point out that certain premises of the dual origin theory have received criticism. For instance, Murray, Wise, and Graham (2017) point out the lack of comparative data that allow the interpretation of the successive stages of the growth rings of cortical differentiation (Fig. 1) as stages of evolutionary history, with more differentiated areas constituting modifications that occurred more recently in the evolution of the mammalian cortex. Importantly, it is not necessary to interpret step-wise structural trends in the mammalian cortex as strict evolutionary trends (Preuss & Goldman-Rakic, 1991). Therefore, while some basic premises of the dual origin theory seem to be rooted on concrete quantitative grounds, certain themes and assumptions of the theory, for instance, the strict interpretation of structural trends as evolutionary trends, might require revision.

From a technical point of view, we have defined the dual connectional trends as a division that maximizes the topological similarity between the two splits, since such division co-localizes very well with prior knowledge on the division and arrangement of cortical areas based on the dual origin framework (Pandya et al., 2015) (Fig. 2). Clearly, such a definition does not exclude the potentially tighter correspondence of other network topology structures with the predictions of the dual origin framework. Investigation of the topological similarity division that we currently used with other network topologies, such as modularity (Shen, Bezgin, Selvam, McIntosh, & Ryan, 2016), will offer a more comprehensive understanding of the nature of the dual connectional trends from a network topology point of view (for a provisional comparison of results derived from module decomposition and their correspondence with the topological symmetry split, see Fig. S4).

Classic definitions of the duality of the cerebral cortex entail the execution of histological work, that is, cyto-and myeloarchitectonic studies (e.g., Sanides, 1962). Ultimately, such histology-based results should be compared with the connectivity-based duality as currently revealed for the mouse, rat and cat cortex. In addition, other modalities can also be used to test the predictions of the dual origin theory. Interestingly, variability at the structural level, assessed with *in vivo* brain imaging, seems to be structured around the two trends that the dual origin theory highlights (Croxson, Forkel, Cerliani, & Thiebaut de Schotten, 2017).

### 5. Conclusions

Uncovering organizational principles of the cerebral cortex is a central goal in multiple fields of neuroscience. The dual origin of the cerebral cortex is such a principle. We have shown that this dual architecture can be conceived as a

topologically symmetric connectional structure, present in the cortical connectome of different mammalian species. This dual structure is also reflected in the spatial dimension of the cortex, resulting in spatially ordered constellations that are centered around the paleocortex and archicortex. Moreover, the dual architecture constitutes a major axis of organization of the transcriptome and reflects the expression of different morphogens stemming from distinct patterning centers in the developing pallium. The ontogeny of this dual connectional structure might be rooted in heterochronous neurodevelopmental gradients in the developing pallium. In sum, the current results exemplify the duality of the cerebral cortex as an overarching organizational principle, reflected across different levels of architecture and across different species, thus constituting one of the major axes of organization of the cerebral cortex.

### CRediT authorship contribution statement

**Alexandros Goulas** Conceptualization, Formal analysis, Funding acquisition, Investigation, Methodology, Project administration, Software, Visualization, Writing - original draft, Writing - review & editing . **Daniel S. Margulies** Formal analysis, Investigation, Visualization, Writing - review & editing . **Gleb Bezgin** Investigation, Software, Visualization, Writing - review & editing . **Claus C. Hilgetag** Funding acquisition, Resources, Supervision, Writing - review & editing .

### Acknowledgements

Support by a Humboldt Research Fellowship from the Alexander von Humboldt Foundation (A.G.) as well as grants from DFG SFB 936/A1, Z3, and TRR 169/A2 (C.C.H.) is gratefully acknowledged.

### Supplementary data

Supplementary data to this article can be found online at <https://doi.org/10.1016/j.cortex.2019.03.002>.

### REFERENCES

- Abbie, A. A. (1940). Cortical lamination in the monotremata. *Journal of Comparative Neurology*, 72, 429–467.
- Abbie, A. A. (1942). Cortical lamination in a polyprotodont marsupial, *Perameles nasuta*. *Journal of Comparative Neurology*, 76, 506–536.
- Aboitiz, F., & Montiel, J. F. (2015). Olfaction, navigation, and the origin of isocortex. *Frontiers in Neuroscience*, 9, 402.
- Aslan, B., & Zech, G. (2005). Statistical energy as a tool for binning-free multivariate goodness-of-fit tests, two-sample comparison and unfolding. *Nuclear Instruments and Methods in Physics Research Section A: Accelerators, Spectrometers, Detectors and Associated Equipment*, 537, 626–636.
- Barbas, H. (1986). Pattern in the laminar origin of corticocortical connections. *Journal of Comparative Neurology*, 252, 415–422.
- Barbas, H., & Pandya, D. N. (1989). Architecture and intrinsic connections of the prefrontal cortex in the rhesus monkey. *Journal of Comparative Neurology*, 286, 353–375.
- Bayer, S. A., & Altman, J. (1987). Directions in neurogenetic gradients and patterns of anatomical connections in the telencephalon. *Progress in Neurobiology*, 29, 57–106.
- Bernard, A., Lubbers, L. S., Tanis, K. Q., Luo, R., Podtelezhnikov, A. A., Finney, E. M., et al. (2012). Transcriptional architecture of the primate neocortex. *Neuron*, 73, 1083–1099.
- Bezgin, G., Rybacki, K., van Opstal, A. J., Bakker, R., Shen, K., Vakorin, V. A., et al. (2014). Auditory-prefrontal axonal connectivity in the macaque cortex: Quantitative assessment of processing streams. *Brain and Language*, 135, 73–84.
- Borello, U., & Pierani, A. (2010). Patterning the cerebral cortex: Traveling with morphogens. *Current Opinion in Genetic Development*, 20, 408–415.
- Bota, M., Talpalaru, S., Hintiryan, H., Dong, H. W., & Swanson, L. W. (2014). BAMS2 workspace: A comprehensive and versatile neuroinformatic platform for collating and processing neuroanatomical connections. *Journal of Comparative Neurology*, 522, 3160–3176.
- Brockhaus, H. (1940). Die Cyto-und Myeloarchitektonik des Cortex claustralis und des Claustrum beim Menschen. *Journal für Psychologie und Neurologie*, 49, 249–348.
- Burt, J. B., Demirtaş, M., Eckner, W. J., Navejar, N. M., Ji, J. L., Martin, W. J., et al. (2018). Hierarchy of transcriptomic specialization across human cortex captured by structural neuroimaging topography. *Nature Neuroscience*, 21, 1251–1259.
- Caviness, V. S., Takahashi, T., & Nowakowski, R. S. (1995). Numbers, time and neocortical neurogenesis: A general developmental and evolutionary model. *Trends in Neurosciences*, 18, 379–383.
- Charvet, C. J., & Finlay, B. L. (2014). Evo-devo and the primate isocortex: The central organizing role of intrinsic gradients of neurogenesis. *Brain, Behavior and Evolution*, 84, 81–92.
- Cipolloni, P. B., & Pandya, D. N. (1999). Cortical connections of the frontoparietal opercular areas in the rhesus monkey. *Journal of Comparative Neurology*, 403, 431–458.
- Croxson, P. L., Forkel, S. J., Cerliani, L., & Thiebaut de Schotten, M. (2017). Structural variability across the primate brain: A cross-species comparison. *Cerebral Cortex*, 28, 3829–3841.
- Dart, R. A. (1934). The dual structure of the neopallium: Its history and significance. *Journal of Anatomy*, 69, 3–19.
- Dong, H. W. (2008). Allen reference atlas: A digital color brain atlas of the C57BL/6J male mouse. Hoboken (New Jersey): John Wiley & Sons.
- Fruchterman, T. M. J., & Reingold, E. M. (1991). Graph drawing by force-directed placement. *Software – Practice & Experience*, 21, 1129–1164.
- Fulcher, B. D., & Fornito, A. (2016). A transcriptional signature of hub connectivity in the mouse connectome. *Proceedings of the National Academy of Science USA*, 113, 1435–1440.
- Fulcher, B. D., Murray, J. D., Zerbi, V., & Wang, X.-J. (2019). Multimodal gradients across mouse cortex. *Proceedings of the National Academy of Science USA*. <https://doi.org/10.1073/pnas.1814144116>.
- García-Cabezas, M.Á., Zikopoulos, B., & Barbas, H. (2019). The structural model: A theory linking connections, plasticity, pathology, development and evolution of the cerebral cortex. *Brain Structure & Function*. <https://doi.org/10.1007/s00429-019-01841-9>.
- Giaccio, R. G. (2006). The dual origin hypothesis: An evolutionary brain-behavior framework for analyzing psychiatric disorders. *Neuroscience and Biobehavioral Reviews*, 30, 526–550.

- Goulas, A., Betzel, R. F., & Hilgetag, C. C. (2018). Spatiotemporal ontogeny of brain wiring. <https://doi.org/10.1101/385369>. bioRxiv.
- Goulas, A., Zilles, K., & Hilgetag, C. C. (2018). Cortical gradients and laminar projections in mammals. *Trends in Neurosciences*, 41, 755–788.
- Grange, P., Bohland, J. W., Hawrylycz, M., & Mitra, P. P. (2012). Brain gene expression analysis: A MATLAB toolbox for the analysis of brain-wide gene-expression data. *ArXiv:1211.6177*.
- Hawrylycz, M. J., Lein, E. S., Guillozet-Bongaarts, A. L., Shen, E. H., Ng, L., Miller, J. A., et al. (2012). An anatomically comprehensive atlas of the adult human brain transcriptome. *Nature*, 489, 391–399.
- Huntenburg, J. M., Bazin, P.-L., Goulas, A., Tarif, C. L., Villringer, A., & Margulies, D. S. (2017). A systematic relationship between functional connectivity and intracortical myelin in the human cerebral cortex. *Cerebral Cortex*, 27, 981–997.
- Kaiser, M. (2017). Mechanisms of connectome development. *Trends in Cognitive Science*, 21, 703–717.
- Kaiser, M., & Hilgetag, C. C. (2007). Development of multi-cluster cortical networks by time windows for spatial growth. *Neurocomputing*, 70, 1829–1832.
- Kaiser, M., Hilgetag, C. C., & van Ooyen, A. (2009). A simple rule for axon outgrowth and synaptic competition generates realistic connection lengths and filling fractions. *Cerebral Cortex*, 19, 3001–3010.
- Kamada, T., & Kawai, S. (1989). An algorithm for drawing general undirected graphs. *Information Processing Letters*, 31, 7–15.
- Lein, E. S., Hawrylycz, M. J., Ao, N., Ayres, M., Bensinger, A., Bernard, A., et al. (2007). Genome-wide atlas of gene expression in the adult mouse brain. *Nature*, 445, 168–176.
- Margulies, D. S., Ghosh, S. S., Goulas, A., Falkiewicz, M., Huntenburg, J. M., Langs, G., et al. (2016). Situating the default-mode network within a principle gradient of macroscale cortical organization. *Proceedings of the National Academy of Science USA*, 113, 12574–12579.
- Markov, N. T., Ercsey-Ravasz, M. M., Ribeiro Gomes, A. R., Lamy, C., Magrou, L., Vezoli, J., et al. (2014). A weighted and directed interareal connectivity matrix for macaque cerebral cortex. *Cerebral Cortex*, 24, 17–36.
- Mishkin, M., & Ungerleider, L. G. (1982). Contribution of striate inputs to the visuospatial functions of parieto-preoccipital cortex in monkeys. *Behavioral and Brain Research*, 6, 57–77.
- Morecraft, R. J., Cipolloni, P. B., Stilwell-Morecraft, K. S., Gedney, M. T., & Pandya, D. N. (2004). Cytoarchitecture and cortical connections of the posterior cingulate and adjacent somatosensory fields in the rhesus monkey. *Journal of Comparative Neurology*, 469, 37–69.
- Murray, E. A., Wise, S. P., & Graham, K. S. (2017). *The evolution of memory systems*. Oxford University Press.
- Nisbach, F., & Kaiser, M. (2007). Developmental time windows for spatial growth generate multiple-cluster small-world networks. *The European Physical Journal B*, 58, 185–191.
- O'Leary, D. D., Chou, S. J., & Sahara, S. (2007). Area patterning of the mammalian cortex. *Neuron*, 56, 252–269.
- Oh, S. W., Harris, J. A., Ng, L., Winslow, B., Cain, N., Mihalas, S., et al. (2014). A mesoscale connectome of the mouse brain. *Nature*, 508, 207–214.
- Pandya, D., Petrides, M., Seltzer, B., & Cipolloni, B. P. (2015). *Cerebral cortex: Architecture, connections, and the dual origin concept*. Oxford Press.
- Pandya, D. N., Seltzer, B., & Barbas, H. (1988). Input-output organization of the primate cerebral cortex. *Neurosciences*. In H. D. Steklis, & J. Erwin (Eds.). *Comparative primate biology* (Vol. 4, pp. 39–80). New York: Alan R Liss.
- Pandya, D. N., & Yeterian, E. H. (1985). Architecture and connections of cortical association areas. In A. Peters, & E. G. Jones (Eds.), *Association and auditory cortices* (pp. 3–61). New York: Springer Science Business Media.
- Pandya, D. N., & Yeterian, E. H. (1990). Prefrontal cortex in relation to other cortical areas in rhesus monkey: Architecture and connections. In H. B. M. Uylings, C. G. Van Eden, J. P. C. De Bruin, M. A. Corner, & M. G. P. Feenstra (Eds.), *The Prefrontal its structure, function and cortex pathology* (Vol. 85, pp. 63–94). Elsevier.
- Pattabiraman, K., Golonzha, O., Lindtner, S., Nord, A. S., Taher, L., Hoch, R., et al. (2014). Transcriptional regulation of enhancers active in protodomains of the developing cerebral cortex. *Neuron*, 82, 989–1003.
- Preuss, T. M., & Goldman-Rakic, P. S. (1991). Myelo- and cytoarchitecture of the granular frontal cortex and surrounding regions in the strepsirrhine primate *Galago* and the anthropoid primate *Macaca*. *Journal of Comparative Neurology*, 310, 429–474.
- Romanski, L. M., Tian, B., Fritz, J., Mishkin, M., Goldman-Rakic, P. S., & Rauschecker, J. P. (1999). Dual streams of auditory afferents target multiple domains in the primate prefrontal cortex. *Nature Neuroscience*, 2, 1131–1136.
- Sanides, F. (1962). *Die Architektonik des menschlichen Stirnhirns*. Berlin-Heidelberg: Springer-Verlag.
- Sanides, F. (1970). Functional architecture of motor and sensory cortices in primates in the light of a new concept of neocortex evolution. In C. R. Noback, & W. Montagna (Eds.), *The primate brain: Advances in primatology* (pp. 137–208). New York: Appleton-Century-Crofts Educational Division/Meredith Corporation.
- Sanides, F., & Hoffmann, J. (1969). Cyto- and myeloarchitecture of the visual cortex of the cat and of the surrounding integration cortices. *Journal für Hirnforschung*, 11, 79–104.
- Scannell, J. W., Blakemore, C., & Young, M. P. (1995). Analysis of connectivity in the cat cerebral cortex. *Journal of Neuroscience*, 15, 1463–1483.
- Shellshear, J. L. (1929). A study of the arteries of the brain of the spiny anteater (*Echidna aculeata*) to illustrate the principles of arterial distribution. *Philosophical Transactions of the Royal Society of London B*, 218, 1–36.
- Shen, K., Bezgin, G., Selvam, R., McIntosh, A. R., & Ryan, J. D. (2016). An anatomical interface between memory and oculomotor systems. *Journal of Cognitive Neuroscience*, 28, 1772–1783.
- Smart, I. H. M. (1984). Histogenesis of the mesocortical area of the mouse telencephalon. *Journal of Anatomy*, 138, 537–552.
- Swanson, L. W. (2004). *Brain maps: Structure of the rat brain. A laboratory guide with printed and electronic templates for data, models and schematics* (3rd ed.). Amsterdam: Elsevier.
- Tiberi, T., Vanderhaeghen, P., & van den Ameele, J. (2012). Cortical neurogenesis and morphogens: Diversity of cues, sources and functions. *Current Opinion in Cell Biology*, 24, 269–276.
- von Bonin, G., & Bailey, P. (1961). Pattern of the cerebral isocortex. In *Primateologia*, Vol. 2, Part 2, Chapter 10. Basel, New York: S. Karger.
- Ypma, R. J. F., & Bullmore, E. T. (2016). Statistical analysis of tract-tracing experiments demonstrates a dense, complex cortical network in the mouse. *PLoS Computational Biology*, 12, e1005104.
- Zingg, B., Hintiryan, H., Gou, L., Song, M. Y., Bay, M., Bienkowski, M. S., et al. (2014). Neural networks of the mouse neocortex. *Cell*, 156, 1096–1111.